Learning to Explain Graph Neural Networks

Giuseppe Serra¹, Mathias Niepert²

¹ School of Computer Science, University of Birmingham

Abstract

Graph Neural Networks (GNNs) are a popular class of machine learning models. Inspired by the learning to explain (L2X) paradigm, we propose L2xGNN, a framework for explainable GNNs which provides faithful explanations by design. L2xGNN learns a mechanism for selecting explanatory subgraphs (motifs) which are exclusively used in the GNNs message-passing operations. L2xGNN is able to select, for each input graph, a subgraph with specific properties such as being sparse and connected. Imposing such constraints on the motifs often leads to more interpretable and effective explanations. Experiments on several datasets suggest that L2xGNN achieves the same classification accuracy as baseline methods using the entire input graph while ensuring that only the provided explanations are used to make predictions. Moreover, we show that L2xGNN is able to identify motifs responsible for the graph's properties it is intended to predict.

Introduction

Graph Neural Networks (GNNs) are a widely used class of machine learning models. Since graphs occur naturally in several domains such as chemistry, biology, and medicine, GNNs have experienced widespread adoption. Following a trend towards building more interpretable machine learning models, there have been numerous recent proposals to provide explanations for GNNs. Most of the existing approaches provide post-hoc explanations starting from an already trained GNN to identify edges and node attributes that explain the model's prediction. However, as highlighted in Faber, K. Moghaddam, and Wattenhofer (2021), there might be some discrepancy between the ground-truth explanations and those attributed to the trained GNNs. Indeed, post-hoc explanations are often not able to faithfully represent the mechanisms of the original model (Rudin 2018). Unfortunately, the very definition of what constitutes a faithful explanation is still open to debate and there exist several competing positions on the matter. Recent work has also shown that post-hoc attribution methods are often not better than random baselines on the standard evaluation metrics for explanation accuracy and faithfulness (Agarwal, Zitnik, and Lakkaraju 2022). A notable exception to a large number of post-hoc XAI methods is PROTGNN (Zhang et al. 2021) which uses prototype-based learning.

A recently proposed alternative to post-hoc methods is the learning to explain (L2X) paradigm (Chen et al. 2018). The

core difference to post-hoc methods is that the models are trained to, in the forward pass, discretely select a small subset of the input features as well as the parameters of a downstream model that uses only the selected features to make a prediction. The selected features are, therefore, faithful by design as they are the only ones used by the downstream model. Since the subset of features is sampled discretely, L2X requires a method for computing gradients of an expectation over a discrete probability distribution. (Chen et al. 2018) proposed a gradient estimator based on a relaxation of the discrete samples and tailored to the k-subset distribution.

With this work, we bring the L2X paradigm to graph representation learning. The important ingredient is a recently proposed method for computing gradients of an expectation over a complex exponential family distribution (Niepert, Minervini, and Franceschi 2021). The method facilitates approximate gradient backpropagation for models combining continuously differentiable GNNs with a black-box solver of combinatorial problems defined on graphs. Crucially, this allows us to learn to sample subgraphs with beneficial properties such as being connected and sparse. Contrary to prior work, this also creates a dependency between the random variables representing the presence of edges. The proposed framework L2xGNN, therefore, learns to select explanatory subgraph motifs and uses these and only these motifs for its message-passing operations. To the best of our knowledge, this is the first method for learning to explain GNNs. The proposed framework is extensible as it can work with any optimization algorithm for graphs imposing properties on the sampled subgraphs.

We compare two different sampling strategies for obtaining sparse subgraph explanations resulting from two optimization problems on graphs: (1) the maximum-weight k-edge subgraph and (2) the maximum-weight k-edge connected subgraph problem. We show empirically that L2xGNN when combined with a base GNN does not lose accuracy on several benchmark datasets. Moreover, we evaluate the explanations quantitatively and qualitatively. We also analyze the ability of L2xGNN to help in detecting shortcut learning which can be used for debugging the GNN. Given the characteristics of the proposed method, our work improves model interpretability and increases the clarity of known black-box models as GNNs while maintaining competitive predictive capabilities.

² Department of Computer Science, University of Stuttgart gxs824@student.bham.ac.uk, mniepert@gmail.com

Background

Let $\mathcal{G}(V,E)$ be a graph with n=|V| the number of nodes. Let $\mathbf{X} \in \mathbb{R}^{n \times d}$ be the feature matrix that associates each node of the graph with a d-dimensional feature vector and let $\mathbf{A} \in \mathbb{R}^{n \times n}$ be the adjacency matrix. GNNs have three computations based on the message passing paradigm (Hamilton, Ying, and Leskovec 2017) which is defined as

$$\mathbf{h}_{i}^{\ell} = \gamma \left(\mathbf{h}_{i}^{\ell-1}, \Box_{j \in \mathcal{N}(v_{i})} \phi \left(\mathbf{h}_{i}^{\ell-1}, \mathbf{h}_{i}^{\ell-1}, r_{ij} \right) \right), \quad (1)$$

where γ , \square , and ϕ represent update, aggregation and message function respectively.

Propagation step. The message-passing network computes a message $m_{ij}^{\ell} = \phi(\mathbf{h}_i^{\ell-1}, \mathbf{h}_j^{\ell-1}, r_{ij})$ between every pair of nodes (v_i, v_j) . The function takes in input v_i 's and v_j 's representations $\mathbf{h}_i^{\ell-1}$ and $\mathbf{h}_j^{\ell-1}$ at the previous layer $\ell-1$, and the relation r_{ij} between the two nodes.

Aggregation step. For each node in the graph, the network performs an aggregation computation over the messages from v_i 's neighborhood $\mathcal{N}(v_i)$ to calculate an aggregated message $M_i^\ell = \Box(\{m_{ij}^\ell \mid v_j \in \mathcal{N}(v_i)\})$. The definition of the aggregation function differs between methods (Hamilton, Ying, and Leskovec 2017; Veličković et al. 2018; Xu et al. 2018; Duval and Malliaros 2021).

Update step. Finally, the model non-linearly transforms the aggregated message M_i^ℓ and v_i 's representation from previous layer $\mathbf{h}_i^{\ell-1}$ to obtain v_i 's representation at layer ℓ as $\mathbf{h}_i^\ell = \gamma(M_i^\ell, \mathbf{h}_i^{\ell-1})$. The final embedding for node v_i after L layers is $\mathbf{z}_i = \mathbf{h}_i^L$ and is used for node classification tasks. For graph classification, an additional readout function aggregates the node representations to obtain a graph representation \mathbf{h}_G . This function can be any permutation invariant function or a graph-level pooling function (Ying et al. 2018; Zhang et al. 2018; Lee, Lee, and Kang 2019). For Graph Isomorphism Networks (GINs) (Xu et al. 2018), for instance, the message passing operation for node v_i is

$$\mathbf{h}_{i}^{\ell} = \gamma^{\ell} \left(\left(1 + \epsilon^{\ell} \right) \cdot \mathbf{h}_{i}^{\ell} + \sum_{j \in \mathcal{N}(v_{i})} \mathbf{h}_{i}^{\ell-1} \right), \tag{2}$$

where γ represents a multi-layer perceptron (MLP), and ϵ denotes a learnable parameter. We will write $\mathbf{H}_{\ell} = \mathrm{GNN}_{\ell}(\mathbf{A},\mathbf{H}_{\ell-1})$ as a shorthand for the application of the ℓ^{th} layer of the GNN under consideration.

Related Work

There are several methods to explain the behavior of GNNs. Following Yuan et al. (2020b), explanatory methods for GNNs can be divided into several categories.

Gradient-based methods. (Pope et al. 2019; Baldassarre and Azizpour 2019; Sanchez-Lengeling et al. 2020). The main idea is to compute the gradients of the target prediction with respect to the corresponding input data. The larger the gradient values, the higher the importance of the input features.

Perturbation-based methods. (Ying et al. 2019; Luo et al. 2020; Funke, Khosla, and Anand 2021; Loveland et al. 2021;

Schlichtkrull, Cao, and Titov 2021; Yuan et al. 2021; Perotti et al. 2022). Here the objective is to study the models' output behavior under input perturbations. When the input is perturbed and we obtain an output comparable to the original one, we can conclude that the perturbed input information is not important for the current input. Inspired by causal inference methods, (Lin, Lan, and Li 2021; Lin et al. 2022; Lucic et al. 2022; Tan et al. 2022) attempt to provide explanations based on factual and counterfactual reasoning.

Surrogate methods. (Huang et al. 2020; Vu and Thai 2020; Duval and Malliaros 2021; Zhang, Defazio, and Ramesh 2021; Gui et al. 2022). First, these approaches generate a local dataset comprised of data points in the neighboring area of the input. The local dataset is assumed to be less complex and, consequently, can be analyzed through a simpler model. Then, a simple and interpretable surrogate model is used to capture local relationships that are used as explanations for the predictions of the original model.

Decomposition methods. (Schwarzenberg et al. 2019; Hu, Li, and Dong 2020; Schnake et al. 2020; Feng et al. 2022). These methods use decomposition rules to decompose the model predictions leading back to the input space. The prediction is considered as the target score. Then, starting from the output layer, the target score is decomposed at each preceding layer according to the decided decomposition rules. In this way, the initial target score is distributed among the neurons at every layer. Finally, the decomposed terms obtained at the input layer are associated to the input features and used as importance scores of the corresponding nodes and edges.

Model-level methods. (Yuan et al. 2020a). Different from the instance-level methods above, these methods provide a general and high-level understanding of the models. In the context of GNNs, they aim at studying the input patterns that would lead to a certain target prediction. The generated explanations are general and provide a global understanding of the trained GNNs.

Prototype-based methods. (Zhang et al. 2021) propose ProtGNN, a new explanatory method based on prototypes to provide *built-in* explanations, overcoming the limitations of post-hoc techniques. The explanations are obtained following case-based reasoning, where new instances are compared with several learned *prototypes*.

Concept-based methods. (Magister et al. 2021) propose CGExplainer, a post-hoc explanatory methods for humanin-the-loop concept discovery. This concept representation learning method extracts concept-based explanations that allow the end-user to analyze predictions with a global view.

Additional works face the explainability problem from different perspectives as explanation supervision (Gao et al. 2021) and motif-based generation (Yu and Gao 2022).

For a comprehensive discussion on methods to explain GNNs, we refer the reader to the survey (Yuan et al. 2020b). Moreover, there have been related methods for learning the structure of graph neural networks (Franceschi et al. 2019) and to sample subgraphs for subgraph aggregation methods (Qian et al. 2022) in a data-driven manner. These methods, however, are not concerned with the problem of explaining the behavior of graph neural networks.

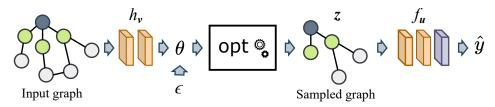


Figure 1: Workflow of the proposed approach.

Limitations of Prior Work

Existing XAI methods for GNNs have several limitations and can lead to inconsistencies (Duval and Malliaros 2021; Faber, K. Moghaddam, and Wattenhofer 2021). We focus on the problem of identifying a subset of the edges as an explanation of the model's message-passing behavior. Hence, an explanation is equivalent to identifying a mask for the adjacency matrix of the original graph. Intuitively, an explanation can be accurate and/or faithful. It is accurate if it succeeds in identifying the edges in the input graph responsible for the graph's class label. This property can, for example, be evaluated with synthetic data where the class label of a graph is determined by the presence or absence of a particular substructure. An explanation is faithful if the edges identified as the explanation cause the prediction of the GNN on an input graph. Contrary to measuring accuracy, there is no consensus on evaluating faithfulness.

Recent work has proposed to measure unfaithfulness as the difference between the predictions of (1) the GNN on a perturbed adjacency matrix and (2) the GNN on the same perturbed adjacency matrix with edges removed by the explanation mask (Pope et al. 2019; Agarwal, Zitnik, and Lakkaraju 2022; Agarwal et al. 2022). We believe that this definition is problematic as the perturbation is typically implemented using a swap operation which replaces two existing edges (a, b) and (c, d) with two new edges (a, c) and (b,d). Hence, these new edges are present in the unmasked adjacency matrix but not present in the masked one. It is, however, natural that the same GNN would predict highly different label distributions on these two graphs. For instance, consider a chemical compound where we remove and add new bonds. The resulting compounds and their properties can be chemically very different. Hence, contrary to prior work, we define a subgraph to be a faithful explanation, if it is a significantly smaller subgraph of the input graph and we know that only its structure is used in the message-passing operations of equation (1).

Learning to Explain Graph Neural Networks

We propose a method that learns both (i) the parameters of a graph generative model and (ii) the parameters of a GNN operating on sparse subgraphs approximately sampled from said generative model in the forward pass. In line with prior work on learning to explain (Chen et al. 2018), the maximum probability subgraph is then used at test time to make the prediction and, therefore, serves as the faithful explanation. Since we aim to sample graphs with certain properties (e.g., connected subgraphs) we need a new approach

to sampling and gradient estimation. Contrary to prior work on edge masking (Schlichtkrull, Cao, and Titov 2021) which treats edges as independent binary random variables, we use a recently introduced method for backpropagating through optimization algorithms. This allows us to select subgraphs with specific properties and, therefore, to explicitly model dependencies between edge variables.

Problem Statement and Framework

We aim to jointly learn the parameters of a probability distribution over subgraphs with certain properties and the parameters of a GNN operating on graphs sampled from said distribution in the context of the graph classification problem. Here, the training data consists of a set of triples $\{(\mathbf{A},\mathbf{X},\mathbf{y})_j\}, j\in\{1,...,N\}$, where \mathbf{A} is an $n\times n$ binary adjacency matrix, $\mathbf{X}\in\mathbf{R}^{n\times d}$ a node attribute matrix with d the number of node attributes, and \mathbf{y} the target graph label. First, we have a learnable function $h_{\mathbf{v}}:\mathcal{A}\times\mathcal{X}\to\Theta$ where \mathcal{A} is the set of all $n\times n$ adjacency matrices, \mathcal{X} the set of all attribute matrices, \mathbf{v} are the parameters of h, and Θ the set of possible edge parameter values. The function, which we refer to as the upstream model, maps the adjacency and attribute matrix to a matrix of edge weights $\mathbf{\theta}\in\mathbb{R}^{n\times x}$. Intuitively, $\mathbf{\theta}_{i,j}$ is the prior probability of edge (i,j).

Next, we assume an algorithm opt : $\Theta \to \mathcal{A}$ which returns the (approximate) solutions to an optimization problem on edge-weighted graphs. Examples of such optimization problems are the maximum-weight spanning tree or the maximum-weight k-edge connected subgraph problems. The optimization algorithm is treated as a black box. One can choose the optimization problem according to the application's requirements. We have found, for instance, that the connected subgraphs lead to better explanations in the domain of chemical compound classification. Contrary to prior work, the optimization problem creates a dependency between the binary variables modeling the edges.

For every binary adjacency matrix $Z \in \mathcal{A}$, we write $Z \in \mathcal{F}$ if and only if the adjacency matrix is a feasible solution (not necessarily an optimal one) of the chosen optimization problem. We can now define a discrete exponential family distribution as

$$p(\mathbf{Z}; \boldsymbol{\theta}) = \begin{cases} \exp(\langle \mathbf{Z}, \boldsymbol{\theta} \rangle_F - B(\boldsymbol{\theta})) & \text{if } \mathbf{Z} \in \mathcal{F}, \\ 0 & \text{otherwise.} \end{cases}$$
(3)

where $\langle \cdot, \cdot \rangle_F$ is the Frobenius inner product and $B(\theta)$ is the log-partition function defined as

$$B(\boldsymbol{\theta}) = \log \left(\sum_{\boldsymbol{A} \in \mathcal{F}} \exp \left(\langle \boldsymbol{Z}, \boldsymbol{\theta} \rangle_F \right) \right).$$

Hence, p is a probability distribution over adjacency matrices that are feasible solutions to the optimization problem under consideration. Each feasible adjacency matrix's probability mass is proportional to the sum of its edge weights. For example, if the optimization problem is the maximum-weight k-edge connected subgraph problem, the distribution assigns a non-zero probability mass to all adjacency matrices of graphs that have k edges and are connected.

Given an optimization problem, we would like to sample exactly from the above probability distribution $p(Z;\theta)$. Unfortunately, this is intractable since computing the log-partition function is in general NP-hard. However, as in prior work (Niepert, Minervini, and Franceschi 2021), we can use perturb-and-MAP (Papandreou and Yuille 2011) to approximately sample from the above distribution as follows. Let $\epsilon \sim \rho(\epsilon)$ be a $n \times n$ matrix of appropriate random variables such as those following the Gumbel distribution. We can then approximately sample an adjacency matrix Z from $p(Z;\theta)$ by computing

$$Z = \mathsf{opt}(\theta + \epsilon).$$

Hence, we can approximately sample by perturbing the edge weights (unnormalized probabilities) θ and by applying the optimization algorithm to these perturbed weights.

In the final part of the model (the downstream model) we use the sampled Z as the input adjacency matrix to a message-passing neural network $f_u : \mathcal{A} \times \mathcal{X} \to \mathcal{Y}$ computing $\hat{y} = f_u(Z, X)$.

In summary, we have the following model architecture for training input data (A, X, y):

$$\theta = h_{v}(A, X)$$
 with $A \in \mathcal{A}, X \in \mathcal{X}$, (4)

$$Z = \operatorname{opt}(\theta + \epsilon)$$
 with $\epsilon \sim \rho(\epsilon), \epsilon \in \mathbb{R}^{n \times n}$, (5)

$$\hat{\mathbf{y}} = f_{\mathbf{u}}(\mathbf{Z}, \mathbf{X})$$
 with $\hat{\mathbf{y}} \in \mathcal{Y}, f_{\mathbf{u}} : \mathcal{A} \times \mathcal{X} \to \mathcal{Y}$. (6)

Figure 1 illustrates the architecture. With $\omega=(u,v)$ the learnable parameters of the model and the target variable y the loss is now defined as:

$$L(\boldsymbol{A}, \boldsymbol{X}, \boldsymbol{y}; \boldsymbol{\omega}) = \mathbb{E}_{\boldsymbol{\epsilon} \sim \rho(\boldsymbol{\epsilon})} [\ell(f_{\boldsymbol{u}}(\boldsymbol{Z}, \boldsymbol{X}), \boldsymbol{y})], \quad (7)$$

with $Z = \text{opt}(\theta + \epsilon)$, $\theta = h_v(A, X)$, and $\ell : \mathcal{Y} \times \mathcal{Y} \to \mathbb{R}^+$ a point-wise loss function. The gradient of L wrt u is

$$\nabla_{\boldsymbol{u}} L(\boldsymbol{A}, \boldsymbol{X}, \boldsymbol{y}; \boldsymbol{\omega}) = \mathbb{E}[\partial_{\boldsymbol{u}} f_{\boldsymbol{u}}(\boldsymbol{Z}, \boldsymbol{X})^{\mathsf{T}} \nabla_{\boldsymbol{v}} \ell(\hat{\boldsymbol{y}}, \boldsymbol{y})]$$

which can be estimated by Monte-Carlo sampling. In contrast, the gradient of L with respect to \boldsymbol{v} is:

$$\nabla_{\boldsymbol{v}} L(\boldsymbol{A}, \boldsymbol{X}, \boldsymbol{y}; \boldsymbol{\omega}) = \partial_{\boldsymbol{v}} h_{\boldsymbol{v}}(\boldsymbol{A}, \boldsymbol{X})^{\mathsf{T}} \nabla_{\boldsymbol{\theta}} L(\boldsymbol{A}, \boldsymbol{X}, \boldsymbol{y}; \boldsymbol{\omega}),$$

where the challenge is to estimate $\nabla_{\boldsymbol{\theta}} L(\boldsymbol{A}, \boldsymbol{X}, \boldsymbol{y}; \boldsymbol{\omega}) = \nabla_{\boldsymbol{\theta}} \mathbb{E}_{\boldsymbol{\epsilon} \sim \rho(\boldsymbol{\epsilon})} [\ell(f_{\boldsymbol{u}}(\boldsymbol{Z}, \boldsymbol{X}), \boldsymbol{y})]$ because $\boldsymbol{Z} = \text{opt}(\boldsymbol{\theta} + \boldsymbol{\epsilon})$ is not continuously differentiable wrt $\boldsymbol{\theta}$. While it would be possible to use the score function estimator, its high variance typically makes it less competitive in practice (Niepert, Minervini, and Franceschi 2021).

Implicit Maximum-Likelihood Learning

The variant of I-MLE we use in this work estimates $\nabla_{\theta} L(A, X, y; \omega)$ by implicitly creating a target distribution $q(Z; \theta')$ using perturbation-based implicit differentiation (Domke 2010). Here, the parameters θ are moved in the

Algorithm 1: Greedy algorithm opt_{con} for the maximum-weight k-edge connected subgraph problem.

```
Input:
```

Input graph $\mathcal{G} = (V, E)$ Number of edges kEdge weights $\boldsymbol{\theta}$ Initialize: $e = \arg\max_{e_{i,j}} \boldsymbol{\theta}_{i,j}$ Set of selected edges $S = \{e\}$ Set of edges adjacent to selected edge $N = \mathcal{N}(e)$ while |S| < k and |N| > 0 do $e = \arg\max_{e_{i,j} \in N} \boldsymbol{\theta}_{i,j}$ $S = S \cup \{e\}$ $N = N \cup \mathcal{N}(e)$

end while

N = N - S

Return: Adjacency matrix Z of the subgraph induced by the set of selected edges S.

direction of $-\nabla_{\mathbf{Z}}\ell(f_{\mathbf{u}}(\mathbf{A},\mathbf{X}),\mathbf{y}))$, the negative gradient of the downstream loss with respect to the sampled adjacency matrix \mathbf{Z} , to construct $\boldsymbol{\theta}'$

$$q(Z; \theta') := p(Z; \theta - \lambda \nabla_{Z} \ell(f_{u}(Z, X), y))$$
(8)

with $Z = \operatorname{opt}(\theta + \epsilon)$ and $\lambda > 0$ the strength of the perturbation. Intuitively, by moving the weights θ into the direction of the negative gradients of Z, the resulting distribution q is more likely to generate samples with a lower downstream loss. We approximate $\nabla_{\theta} L(A, X, y; \omega)$ with a single-sample Monte Carlo estimate of the gradients of the KL divergence between p and q:

$$\nabla_{\boldsymbol{\theta}} L(\boldsymbol{A}, \boldsymbol{X}, \boldsymbol{y}; \boldsymbol{\omega}) \approx \frac{1}{\lambda} \left(\mathsf{opt}(\boldsymbol{\theta} + \boldsymbol{\epsilon}) - \mathsf{opt}(\boldsymbol{\theta}' + \boldsymbol{\epsilon}) \right).$$
 (9)

In other words, $\nabla_{\theta}L(\boldsymbol{A}, \boldsymbol{X}, \boldsymbol{y}; \boldsymbol{\omega})$ is approximated by the difference between an approximate sample from $p(\boldsymbol{Z}; \boldsymbol{\theta})$ and an approximate sample from $q(\boldsymbol{Z}; \boldsymbol{\theta}')$. In this way we move the distribution $p(\boldsymbol{Z}; \boldsymbol{\theta})$ closer to $q(\boldsymbol{Z}; \boldsymbol{\theta}')$. For further details on I-MLE we refer the reader to the original paper (Niepert, Minervini, and Franceschi 2021).

L2xGNN: Learning to Explain GNNs with I-MLE

We now describe the class of L2xGNN models we use in the experiments. First, we need to define the function $h_{\boldsymbol{v}}(\boldsymbol{A},\boldsymbol{X})$. Here we use a standard GNN (see equation 1) to compute for every node i and every layer ℓ the vector representation $\mathbf{h}_i^\ell = h_{\boldsymbol{v}}(\boldsymbol{A},\boldsymbol{X})_{i,1:d}$. We then compute the matrix of edge weights by taking the inner product between each pair of node embeddings. More formally, we compute $\boldsymbol{\theta}_{i,j} = \langle \mathbf{h}_i^\ell, \mathbf{h}_j^\ell \rangle$ for some fixed ℓ . Typically, we choose $\ell=1$.

In this work, we sample the noise perturbations ϵ from the sum of Gamma distribution (Niepert, Minervini, and Franceschi 2021). Other noise distributions such as the Gumbel distribution are possible.

Table 1: Prediction test accuracy for graph classification tasks. Standard deviations are over ten runs.

| Dataset | | GCN | | GIN | | | |
|-----------------|----------------------|-----------------------|-------------------|-------------------|-----------------------|-------------------|--|
| Butuset | Original | L2xGnn $_{w/o_{con}}$ | L2xGnn | Original | L2xGnn $_{w/o_{con}}$ | L2xGnn | |
| DD | 0.720 ± 0.024 | 0.719 ± 0.031 | 0.719 ± 0.036 | 0.722 ± 0.027 | 0.739 ± 0.051 | 0.720 ± 0.030 | |
| MUTAG | 0.734 ± 0.083 | 0.739 ± 0.111 | 0.745 ± 0.082 | 0.827 ± 0.051 | 0.814 ± 0.092 | 0.825 ± 0.078 | |
| IMDB-B | 0.731 ± 0.032 | 0.660 ± 0.054 | 0.734 ± 0.047 | 0.721 ± 0.050 | 0.650 ± 0.050 | 0.724 ± 0.045 | |
| IMDB-M | 0.500 ± 0.028 | 0.503 ± 0.032 | 0.490 ± 0.022 | 0.490 ± 0.047 | 0.488 ± 0.032 | 0.479 ± 0.035 | |
| PROTEINS | 0.718 ± 0.044 | 0.711 ± 0.034 | 0.720 ± 0.053 | 0.708 ± 0.045 | 0.685 ± 0.029 | 0.709 ± 0.034 | |
| YEAST | 0.881 ± 0.001 | 0.882 ± 0.002 | 0.881 ± 0.001 | 0.883 ± 0.001 | 0.882 ± 0.001 | 0.880 ± 0.002 | |

Sampling constrained subgraphs. An advantage of the proposed method is its ability to integrate any graph optimization problem as long as there exists an algorithm opt for computing (approximate) solutions. In this work, we focus on two optimization problems: (1) The maximumweight k-edge subgraph and (2) the maximum-weight kedge connected subgraph problems. The former aims to find a maximum-weight subgraph with k edges. The latter aims to find a connected maximum-weight subgraph with k edges. Other optimization problems are possible but we found that sparse and connected subgraphs provide a good efficiency-effectiveness trade-off.

Computing maximum weight k-edge subgraphs is highly efficient as we only need to select the k edges with the maximum weights. In order to compute connected k-edge subgraphs we use a greedy approach. First, given a number k of edges, we select a single edge $e_{i,j}$ with the highest weight $\theta_{i,j}$ from the input graph. At every iteration of the algorithm, we select the next edge such that it (a) is connected to a previously selected edge and (b) has the maximum weight among all those connected edges. A more detailed description of the greedy algorithm is given in Algorithm 1.

Finally, we need to define the function f_{u} (the downstream function) of the proposed framework. Here, we again use a message-passing GNN that follows the update rule

$$\mathbf{h}_{i}^{\ell} = \gamma \left(\mathbf{h}_{i}^{\ell-1}, \Box_{j \in \mathcal{N}(v_{i})} \phi \left(\mathbf{h}_{i}^{\ell-1}, \mathbf{h}_{j}^{\ell-1}, r_{ij} \right) \right). \tag{10}$$

The neighborhood structure $\mathcal{N}(\cdot)$, however, is defined through the output adjacency matrix Z of the optimization algorithm opt

$$j \in \mathcal{N}(v_i) \iff \mathbf{Z}_{i,j} = \mathbf{Z}_{j,i} = 1.$$
 (11)

Hence, if after the subgraph sampling, there exists a node v_i which is an isolated node in the adjacency matrix Z, that is, $Z_{i,j} = Z_{j,i} = 0 \ \forall j \in \{1,...,n\}$, the embedding of the node will not be updated based on message passing steps with neighboring nodes. This means that, for *isolated* nodes, the only information used in the downstream model is the one from the nodes themselves. Conceptually, Z works as a mask over the messages m_{ij}^ℓ computed at each layer ℓ . The adjacency matrix \boldsymbol{Z} is then used in all subsequent

layers of the GNN. In particular, for one layer ℓ we have

$$\mathbf{H}_{\ell} = \operatorname{GNN}_{\ell}(\boldsymbol{A} \odot \boldsymbol{Z}, \mathbf{H}_{\ell-1}), \tag{12}$$

where \odot is the Hadamard product. Finally, the remaining part of the L2xGNN network for the graph classification is

$$\mathbf{h}_G = \text{Pool}(\mathbf{H}_\ell) \qquad \hat{\mathbf{y}} = \eta(\mathbf{h}_G), \tag{13}$$

where we use a global pooling operator to generate the (sub)graph representation h_G that will then be used by the MLP network $\eta(\cdot)$ to output a probability distribution \hat{y} over the class labels. Finally, a loss function is applied whose gradients are used to perform backpropagation. At test time, we use the maximum-probability subgraph for the explanation and prediction, that is, we do not perturb at test time.

Experiments

First, we evaluate the predictive performance of the model compared to baselines. Second, we qualitatively and quantitatively analyze the explanatory subgraphs for datasets for which we know the ground-truth motifs. Finally, we perform several ablation studies to investigate the effects of different model choices on the results.

Datasets and Settings

Datasets. To understand the change in the predictive capabilities of the base models when integrating L2xGNN, we use six real-world datasets for graph classification tasks: MUTAG (Debnath et al. 1991), PROTEINS (Borgwardt et al. 2005), YEAST (Yan et al. 2008), IMBD-BINARY, IMBD-MULTI (Yanardag and Vishwanathan 2015), and DD (Rossi and Ahmed 2015). To quantitatively evaluate the quality of the explanations, we use datasets that include ground-truth edge masks. In particular, we use MUTAG₀ and BA2Motifs. $MUTAG_0$ is a dataset introduced in Tan et al. (2022) which contains the benzene-NO2 (i.e., a carbon ring with a nitro group (NO₂) attached) as the only discriminative motif between positive and negative labels. BA2Motifs is a synthetic dataset that was first introduced in Luo et al. (2020). The base graphs are Barabasi-Albert (BA) graphs. 50% of the graphs are augmented with a house-motif graphs, the rest with a 5-node cycle motif. The discriminative subgraph leading to different predictions is the motif attached to the BA graph.

Experimental settings. To evaluate the quality of our approach, we use L2xGNN with several GNN base models including GCN (Kipf and Welling 2017) and GIN (Xu

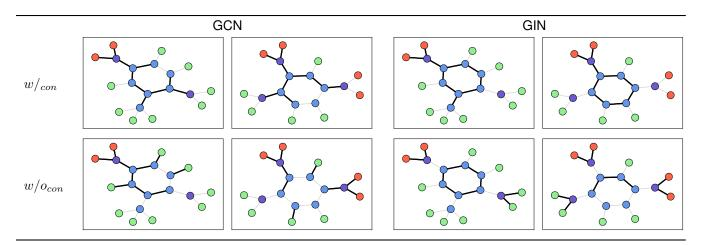


Figure 2: Visualization of some of the subgraphs selected by L2xGNN for MUTAG $_0$ on the test set. The solid edges are the ones sampled by our approach. The first and second rows depict, respectively, some motifs with or without constraining the subgraphs to be connected. Blue, purple, red, and green nodes represent carbon (C), nitrogen (N), oxygen (O), and hydrogen (H) atoms respectively.

et al. 2018). We compare the results when using the original model and when the same model is combined with our XAI method. For model selection and evaluation, to fairly compare the methods, we follow a previously proposed protocol¹. The hyperparameter selection is performed via 10-fold cross-validation, where a training fold is randomly used as a validation set. The selection is performed for the number of layers [1, 2, 3, 4] and the number of hidden units [16, 32, 64, 128] based on the validation accuracy. For a fair comparison with the backbone architectures, we select the best configuration for each dataset, and we integrate our approach into the best model. Instead of fixing a value k for each input graph, we compute k based on a ratio R of edges to be kept. Once the hyperparameters of the default model are found, we select the best ratio R from the set of values [0.4, 0.5, 0.6, 0.7] based on the validation accuracy. We do not include extreme values for two reasons: (1) smaller values for R lead to reduced predictive capabilities and do not lead to meaningful explanatory subgraphs; and (2) higher values would not remove enough edges compared to the original input. Finally, we choose the perturbation intensity λ from the values [10, 100, 1000].

Empirical Results

Graph Classification Comparison with Base GNNs. Following the experimental procedure proposed in Zhang et al. (2021), Table 1 lists the results of using L2xGNN with base GNN architectures for graph classification tasks. We observe that L2xGNN is competitive and sometimes even outperforms the base GNN models on the benchmark datasets. Note that the primary goal of this work is not to provide a better predictive model, but to provide faithful explanation masks while maintaining similar predictive capabilities.

Explanation Accuracy. We compare the proposed method with popular post-hoc explanation techniques including the GNN-Explainer (Ying et al. 2019), PGE-Explainer (Luo et al. 2020), GradCAM (Pope et al. 2019) and SubgraphX (Yuan et al. 2021)². We train a 3-layer GIN for 200 epochs with hidden dimensions equal to 64 and a learning rate equal to 0.001. We save the best model according to the validation accuracy and we compare it with the post-hoc techniques. In our case, we integrate L2xGNN into the same architecture and learn the edge masking during training as described before. In Table 2, we report the explanation accuracy evaluation with respect to the ground-truth motifs in comparison with post-hoc techniques. The explanation problem is formalized as a binary classification problem, where the edges belonging to the ground-truth motif are treated as positive labels. We observe that L2xGNN obtains better or the same results as the baseline GNN models. While for the post-hoc explanation techniques we cannot guarantee that the GNNs use exclusively the explanation subgraphs for the prediction (Yuan et al. 2020b), our method, by providing faithful explanations, overcomes this limitation. It is exactly the provided explanation that is used in the message-passing operations of L2xGNN.

Qualitative Evaluation of the Explanations. In Figure 2, we present some of the subgraphs identified by L2xGNN when combined with two different base GNNs. Based on prior studies and chemical domain knowledge (Debnath et al. 1991; Lin, Lan, and Li 2021; Tan et al. 2022), carbon rings (the blue circles in the pictures) and NO₂ groups are known to be mutagenic. Interestingly, we can notice that, when using the information of connected subgraphs, the models are able to recognize a complete carbon ring with a NO₂ group in most of the cases. In some cases, the carbon

¹https://github.com/pyg-team/pytorch_geometric/tree/master/benchmark/kernel

²Implementations taken from the DIG library (Liu et al. 2021).

Table 2: Evaluation of explanations on synthetic graph classification datasets using a 3-layer GIN architecture.

| Dataset | BA-2MOTIFS | | | | $MUTAG_0$ | | | |
|--------------------|------------|------|------|-------|-----------|------|------|-------|
| | Acc. | Pr. | Rec. | F_1 | Acc. | Pr. | Rec. | F_1 |
| GNN-Exp. | .614 | .328 | .658 | .425 | .492 | .415 | .548 | .452 |
| GradCAM | .816 | .534 | .925 | .674 | .722 | .733 | .554 | .608 |
| PGE-Exp. | .588 | .313 | .673 | .417 | .731 | .682 | .661 | .657 |
| SubgraphX | .847 | .640 | .920 | .738 | .725 | .765 | .497 | .583 |
| L2xGnn | .837 | .580 | .900 | .704 | .794 | .706 | .891 | .762 |
| L2xGnn w/o_{con} | .818 | .549 | .942 | .690 | .720 | .628 | .828 | .689 |

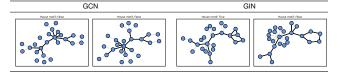


Figure 3: Example of model analysis based on the generated explanations.

ring is not complete, but the explanations are still helpful to understand which motifs are potentially important for the prediction. In the second row, we can observe the results of the sampling strategy where we do not require subgraphs to be connected. In this case, the carbon rings are not always identified. Instead, the NO₂ group is always considered important for the prediction. More generally, as also reported in Yuan et al. (2021), studying connected subgraphs results in more natural motifs compared to the motifs obtained without the connectedness constraint.

Shortcut Learning Detection. By generating *faithful* subgraph explanations, our approach can be used to detect whether the predictive model is focusing on the expected features or if it is affected by shortcut learning. This is particularly important for GNNs, where seemingly small implementation differences can influence the learning process of the model (Schlichtkrull, Cao, and Titov 2021). To this end, we use the BA2Motifs dataset (Luo et al. 2020). We trained two different models, GCN and GIN, achieving a test accuracy of 0.67 and 1.0 respectively. Taking a closer look at the explanations of the first model, we observed that most of the correct predictions were (incorrectly) correlated with the cycle motif and that the explanations were similar to the ones reported in Figure 3. The explanatory results show that the model is not learning the expected discriminative motifs and, consequently, the accuracy for the test set is poor. This insight can help users to change the configuration of the architecture or to use a different model (e.g., GIN). More generally, the results highlight that faithful explanations can facilitate model analysis and debugging.

Ablation Studies. In Table 1, we compare the two sampling strategies. From the results, the connected sampling is able to get better results than the non-connected counterpart on most datasets. In fact, the connectivity of subgraphs is essential to grasp the complete information about the important patterns, especially for chemical compound data where connected atoms are usually expected to create molecules

Table 3: Effect of the edge ratio on the prediction accuracy.

| Ratio | 0.2 | 0.3 | 0.4 | 0.5 | 0.6 | 0.7 | 0.8 | 0.9 | |
|------------|--------------|--------------|--------------|--------------|--------------|--------------|--------------|--------------|--|
| | | MUTAG | | | | | | | |
| GCN GIN | .696 .786 | .708 .808 | .713 .814 | .739 .823 | .724 .824 | .729 .808 | .718 .798 | .745 .832 | |
| | | | | PROT | EINS | | | | |
| GCN GIN | .714 .668 | .712 .690 | .723 .691 | .720 .698 | .724 .696 | .727 .703 | .719 .704 | .727 .714 | |

or chemical groups. This aspect is also supported by the results obtained in Table 2, where the connected strategy returns better explanations for the chemical dataset. Additionally, as previously mentioned, evaluating connected structures rather than just important edges looks more natural and intelligible. In Table 3, we analyze the effect of the quantity of retained information on the prediction accuracy. A smaller ratio indicates that we retain fewer edges during training and, consequently, the resulting subgraphs are more sparse and, therefore, interpretable. As one can see, this affects the predictive capabilities only when R is small. Starting from R = 0.5, the ratio does not affect particularly the predictive capabilities of the model. In fact, for graph classification tasks, some of the information contained in the initial computational graph does not condition the prediction as the information may be redundant or noisy. For instance, considering the MUTAG dataset, we know that the initial graphs contain on average 20 edges. The discriminative motif benzene-NO₂, instead, contains around 9 edges, meaning that we ideally need 50% of the original edges to obtain good results. This is in line with the findings of this analysis and the graph classification results previously reported in Table 1.

Conclusion and Limitations

We propose L2xGNN³, a framework that can be integrated into GNN architectures to learn to generate explanatory subgraphs which are exclusively used for the models' predictions. Our experimental findings demonstrate that the integration of L2xGNN with base GNNs does not affect the predictive capabilities of the model for graph classification tasks. Furthermore, according to the definition provided in the paper, the resulting explanations are *faithful* since the retained information is the only one used by the model for prediction. Hence, differently from most of the common techniques, our explanations reveal the rationale of the GNNs and can also be used for model analysis and debugging.

A limitation of the approach is the reduced efficiency compared to baseline GNN models. Since we need to integrate an algorithm to compute (approximate) solutions to a combinatorial optimization problem, each forward-pass requires more time and resources. Moreover, depending on the choice of the optimization problem, we might not capture the structure of explanatory motifs required for the application under consideration.

³Code: https://github.com/GiuseppeSerra93/L2XGNN

References

- Agarwal, C.; Queen, O.; Lakkaraju, H.; and Zitnik, M. 2022. An Explainable AI Library for Benchmarking Graph Explainers.
- Agarwal, C.; Zitnik, M.; and Lakkaraju, H. 2022. Probing gnn explainers: A rigorous theoretical and empirical analysis of gnn explanation methods. In *International Conference on Artificial Intelligence and Statistics*, 8969–8996.
- Baldassarre, F.; and Azizpour, H. 2019. Explainability techniques for graph convolutional networks. *arXiv preprint arXiv:1905.13686*.
- Borgwardt, K. M.; Ong, C. S.; Schönauer, S.; Vishwanathan, S.; Smola, A. J.; and Kriegel, H.-P. 2005. Protein function prediction via graph kernels. *Bioinformatics*, 21(suppl_1): i47–i56.
- Chen, J.; Song, L.; Wainwright, M.; and Jordan, M. 2018. Learning to explain: An information-theoretic perspective on model interpretation. In *International Conference on Machine Learning*, 883–892. PMLR.
- Debnath, A. K.; Lopez de Compadre, R. L.; Debnath, G.; Shusterman, A. J.; and Hansch, C. 1991. Structure-activity relationship of mutagenic aromatic and heteroaromatic nitro compounds. correlation with molecular orbital energies and hydrophobicity. *Journal of medicinal chemistry*, 34(2): 786–797.
- Domke, J. 2010. Implicit differentiation by perturbation. *Advances in Neural Information Processing Systems*, 23: 523–531.
- Duval, A.; and Malliaros, F. D. 2021. Graphsvx: Shapley value explanations for graph neural networks. In *Joint European Conference on Machine Learning and Knowledge Discovery in Databases*, 302–318. Springer.
- Faber, L.; K. Moghaddam, A.; and Wattenhofer, R. 2021. When Comparing to Ground Truth is Wrong: On Evaluating GNN Explanation Methods. In *Proceedings of the 27th ACM SIGKDD Conference on Knowledge Discovery & Data Mining*, 332–341.
- Feng, Q.; Liu, N.; Yang, F.; Tang, R.; Du, M.; and Hu, X. 2022. DEGREE: Decomposition Based Explanation for Graph Neural Networks. In *International Conference on Learning Representations*.
- Franceschi, L.; Niepert, M.; Pontil, M.; and He, X. 2019. Learning discrete structures for graph neural networks. In *International conference on machine learning*, 1972–1982.
- Funke, T.; Khosla, M.; and Anand, A. 2021. Zorro: Valid, sparse, and stable explanations in graph neural networks. *arXiv* preprint arXiv:2105.08621.
- Gao, Y.; Sun, T.; Bhatt, R.; Yu, D.; Hong, S.; and Zhao, L. 2021. Gnes: Learning to explain graph neural networks. In 2021 IEEE International Conference on Data Mining (ICDM), 131–140. IEEE.
- Gui, S.; Yuan, H.; Wang, J.; Lao, Q.; Li, K.; and Ji, S. 2022. FlowX: Towards Explainable Graph Neural Networks via Message Flows. *arXiv preprint arXiv:2206.12987*.

- Hamilton, W. L.; Ying, R.; and Leskovec, J. 2017. Inductive representation learning on large graphs. In *Proceedings of the 31st International Conference on Neural Information Processing Systems*, 1025–1035.
- Hu, J.; Li, T.; and Dong, S. 2020. GCN-LRP explanation: exploring latent attention of graph convolutional networks. In 2020 International Joint Conference on Neural Networks (IJCNN), 1–8. IEEE.
- Huang, Q.; Yamada, M.; Tian, Y.; Singh, D.; Yin, D.; and Chang, Y. 2020. Graphlime: Local interpretable model explanations for graph neural networks. *arXiv preprint arXiv:2001.06216*.
- Kipf, T. N.; and Welling, M. 2017. Semi-supervised classification with graph convolutional networks. In *International Conference on Learning Representations*.
- Lee, J.; Lee, I.; and Kang, J. 2019. Self-attention graph pooling. In *International conference on machine learning*, 3734–3743. PMLR.
- Lin, W.; Lan, H.; and Li, B. 2021. Generative causal explanations for graph neural networks. In *International Conference on Machine Learning*, 6666–6679. PMLR.
- Lin, W.; Lan, H.; Wang, H.; and Li, B. 2022. OrphicX: A Causality-Inspired Latent Variable Model for Interpreting Graph Neural Networks. *arXiv preprint arXiv:2203.15209*.
- Liu, M.; Luo, Y.; Wang, L.; Xie, Y.; Yuan, H.; Gui, S.; Yu, H.; Xu, Z.; Zhang, J.; Liu, Y.; Yan, K.; Liu, H.; Fu, C.; Oztekin, B. M.; Zhang, X.; and Ji, S. 2021. DIG: A Turnkey Library for Diving into Graph Deep Learning Research. *Journal of Machine Learning Research*, 22(240): 1–9.
- Loveland, D.; Liu, S.; Kailkhura, B.; Hiszpanski, A.; and Han, Y. 2021. Reliable Graph Neural Network Explanations Through Adversarial Training. *arXiv preprint arXiv:2106.13427*.
- Lucic, A.; Ter Hoeve, M. A.; Tolomei, G.; De Rijke, M.; and Silvestri, F. 2022. Cf-gnnexplainer: Counterfactual explanations for graph neural networks. In *International Conference on Artificial Intelligence and Statistics*, 4499–4511. PMLR.
- Luo, D.; Cheng, W.; Xu, D.; Yu, W.; Zong, B.; Chen, H.; and Zhang, X. 2020. Parameterized explainer for graph neural network. *arXiv preprint arXiv:2011.04573*.
- Magister, L. C.; Kazhdan, D.; Singh, V.; and Liò, P. 2021. GCExplainer: Human-in-the-Loop Concept-based Explanations for Graph Neural Networks. *arXiv preprint arXiv:2107.11889*.
- Niepert, M.; Minervini, P.; and Franceschi, L. 2021. Implicit MLE: Backpropagating Through Discrete Exponential Family Distributions. In *NeurIPS*, Proceedings of Machine Learning Research. PMLR.
- Papandreou, G.; and Yuille, A. L. 2011. Perturb-and-MAP random fields: Using discrete optimization to learn and sample from energy models. In *2011 International Conference on Computer Vision*, 193–200.
- Perotti, A.; Bajardi, P.; Bonchi, F.; and Panisson, A. 2022. GRAPHSHAP: Motif-based Explanations for Black-box Graph Classifiers. *arXiv* preprint arXiv:2202.08815.

- Pope, P. E.; Kolouri, S.; Rostami, M.; Martin, C. E.; and Hoffmann, H. 2019. Explainability methods for graph convolutional neural networks. In *Proceedings of the IEEE/CVF Conference on Computer Vision and Pattern Recognition*, 10772–10781.
- Qian, C.; Rattan, G.; Geerts, F.; Morris, C.; and Niepert, M. 2022. Ordered Subgraph Aggregation Networks. *arXiv* preprint arXiv:2206.11168.
- Rossi, R.; and Ahmed, N. 2015. The network data repository with interactive graph analytics and visualization. In *Twenty-ninth AAAI conference on artificial intelligence*.
- Rudin, C. 2018. Stop Explaining Black Box Machine Learning Models for High Stakes Decisions and Use Interpretable Models Instead. Manuscript based on C. Rudin Please Stop Explaining Black Box Machine Learning Models for High Stakes Decisions. In *Proceedings of NeurIPS 2018 Workshop on Critiquing and Correcting Trends in Learning*.
- Sanchez-Lengeling, B.; Wei, J.; Lee, B.; Reif, E.; Wang, P.; Qian, W.; McCloskey, K.; Colwell, L.; and Wiltschko, A. 2020. Evaluating attribution for graph neural networks. *Advances in neural information processing systems*, 33: 5898–5910.
- Schlichtkrull, M. S.; Cao, N. D.; and Titov, I. 2021. Interpreting Graph Neural Networks for {NLP} With Differentiable Edge Masking. In *International Conference on Learning Representations*.
- Schnake, T.; Eberle, O.; Lederer, J.; Nakajima, S.; Schütt, K. T.; Müller, K.-R.; and Montavon, G. 2020. Higher-order explanations of graph neural networks via relevant walks. *arXiv preprint arXiv:2006.03589*.
- Schwarzenberg, R.; Hübner, M.; Harbecke, D.; Alt, C.; and Hennig, L. 2019. Layerwise relevance visualization in convolutional text graph classifiers. *arXiv preprint arXiv:1909.10911*.
- Tan, J.; Geng, S.; Fu, Z.; Ge, Y.; Xu, S.; Li, Y.; and Zhang, Y. 2022. Learning and Evaluating Graph Neural Network Explanations based on Counterfactual and Factual Reasoning. In *Proceedings of the ACM Web Conference* 2022, 1018–1027.
- Veličković, P.; Cucurull, G.; Casanova, A.; Romero, A.; Liò, P.; and Bengio, Y. 2018. Graph Attention Networks. In *International Conference on Learning Representations*.
- Vu, M. N.; and Thai, M. T. 2020. Pgm-explainer: Probabilistic graphical model explanations for graph neural networks. *arXiv preprint arXiv:2010.05788*.
- Xu, K.; Hu, W.; Leskovec, J.; and Jegelka, S. 2018. How Powerful are Graph Neural Networks? In *International Conference on Learning Representations*.
- Yan, X.; Cheng, H.; Han, J.; and Yu, P. S. 2008. Mining significant graph patterns by leap search. In *Proceedings of the 2008 ACM SIGMOD international conference on Management of data*, 433–444.
- Yanardag, P.; and Vishwanathan, S. 2015. Deep graph kernels. In *Proceedings of the 21th ACM SIGKDD international conference on knowledge discovery and data mining*, 1365–1374.

- Ying, R.; Bourgeois, D.; You, J.; Zitnik, M.; and Leskovec, J. 2019. Gnnexplainer: Generating explanations for graph neural networks. *Advances in neural information processing systems*, 32: 9240.
- Ying, Z.; You, J.; Morris, C.; Ren, X.; Hamilton, W.; and Leskovec, J. 2018. Hierarchical graph representation learning with differentiable pooling. *Advances in neural information processing systems*, 31.
- Yu, Z.; and Gao, H. 2022. MotifExplainer: a Motifbased Graph Neural Network Explainer. arXiv preprint arXiv:2202.00519.
- Yuan, H.; Tang, J.; Hu, X.; and Ji, S. 2020a. Xgnn: Towards model-level explanations of graph neural networks. In *Proceedings of the 26th ACM SIGKDD International Conference on Knowledge Discovery & Data Mining*, 430–438.
- Yuan, H.; Yu, H.; Gui, S.; and Ji, S. 2020b. Explainability in graph neural networks: A taxonomic survey. *arXiv preprint arXiv:2012.15445*.
- Yuan, H.; Yu, H.; Wang, J.; Li, K.; and Ji, S. 2021. On explainability of graph neural networks via subgraph explorations. *arXiv preprint arXiv:2102.05152*.
- Zhang, M.; Cui, Z.; Neumann, M.; and Chen, Y. 2018. An end-to-end deep learning architecture for graph classification. In *Proceedings of the AAAI conference on artificial intelligence*, volume 32.
- Zhang, Y.; Defazio, D.; and Ramesh, A. 2021. Relex: A model-agnostic relational model explainer. In *Proceedings of the 2021 AAAI/ACM Conference on AI, Ethics, and Society*, 1042–1049.
- Zhang, Z.; Liu, Q.; Wang, H.; Lu, C.; and Lee, C. 2021. Prot-GNN: Towards Self-Explaining Graph Neural Networks. *arXiv* preprint arXiv:2112.00911.

Dataset Statistics

In Table 4, we report the statistics of the datasets used for graph classification tasks. We use datasets from different domains including biological data, social networks, and bioinformatics data. For a comprehensive evaluation, we include datasets with different characteristics, such as a larger number of graphs or a larger number of nodes and edges.

Table 4: Statistics of the datasets.

| Number of | Nodes (avg) | Edges (avg) | Graphs | Classes |
|-----------|-------------|-------------|--------|---------|
| DD | 284.32 | 715.66 | 1178 | 2 |
| MUTAG | 17.93 | 19.79 | 188 | 2 |
| IMDB-B | 19.77 | 96.53 | 1000 | 2 |
| IMDB-M | 13.00 | 65.94 | 1500 | 3 |
| PROTEINS | 39.06 | 72.82 | 1113 | 2 |
| YEAST | 21.54 | 22.84 | 79601 | 2 |

Hyperparameter Selection

Experiments were run on a single Linux machine with Intel Core i7-11370H @ 3.30GHz, 1 GeForce RTX 3060, and 16 GB RAM. The best hyperparameter configuration for each model and dataset used for graph classification tasks is reported in Table 5.

Table 5: Hyperparameter settings for graph classification tasks.

| | | GC | CN | | GIN | | | |
|-----------------|--------|--------|-----|------|--------|--------|-----|------|
| | Hidden | Layers | R | λ | Hidden | Layers | R | λ |
| DD | 128 | 2 | 0.6 | 10 | 64 | 1 | 0.5 | 100 |
| MUTAG | 128 | 3 | 0.6 | 1000 | 128 | 4 | 0.5 | 10 |
| IMDB-B | 128 | 3 | 0.4 | 100 | 64 | 3 | 0.4 | 1000 |
| IMDB-M | 64 | 3 | 0.6 | 10 | 128 | 4 | 0.6 | 10 |
| PROTEINS | 128 | 3 | 0.7 | 100 | 128 | 4 | 0.5 | 10 |
| YEAST | 128 | 3 | 0.6 | 10 | 128 | 3 | 0.6 | 10 |